Monitoring Global Energy Flow to Primary Production

Dennis G. Dye

Institute of Industrial Science
University of Tokyo
7-22-1 Roppongi, Minato-ku
Tokyo 106, Japan
Fax: +81-3-5411-0441
E-mail: dye@shunji.iis.u-tokyo.ac.jp

Abstract

Global satellite estimates of annual incident and terrestrial vegetation-absorbed photosynthetically active radiation (PAR, 400-700 nm) are evaluated for the 11 years from 1979 to 1989. The data sets were derived from Nimbus-7 Total Ozone Mapping Spectrometer (TOMS) and NOAA Advanced Very High Resolution Radiometer (AVHRR) observations. The mean annual total PAR incident at the Earth's surface between 60°N and 60°S latitudes is estimated to be 1.26 x 10^6 EJ, of which 9.17 x 10^5 EJ (73%) is incident on ocean surfaces and 3.42x 10^5 EJ (27%) is incident on terrestrial surfaces. A 1.7% reduction in northern hemisphere (60°N-0°) incident PAR in 1982 is attributed to changes in cloud amount and distribution associated with El Niño-Southern Oscillation conditions and possibly aerosols from the 1982 El Chichón volcanic eruption. The estimated annual total PAR absorbed by terrestrial vegetation (APAR) between 60°N and 60°S is 1.10 x 10^5 EJ, or 8.8% of total incident PAR (11-year means). The observed patterns of distribution and variability account for the primary flow of energy to global primary production.

1. Introduction

Life processes on Earth, with limited exceptions, are supported by the solar energy that is initially captured through photoautotrophic primary production. This captured energy becomes stored in the chemical bonds of plant biomass and comprises the basic energy reservoir for the planetary food web. Primary production also influences the state and functioning of the biosphere through linkages to physical processes of the Earth system, including the global biogeochemical, hydrological and nutrient cycles.

The amount of PAR energy absorbed by terrestrial vegetation over a particular time interval (APAR, MJ m^{-2}) may be computed as

$$APAR = FAPAR \cdot S, \quad (1)$$

where FAPAR is the fraction of incident PAR absorbed by the photosynthetic elements of the vegetation cover, and S is the total incident PAR (MJ m^{-2}). The term FAPAR is a measure of the capacity of the vegetation in the observed landscape to intercept and absorb incident PAR, and is closely related to green-leaf biomass and leaf area index (LAI). The S term defines the amount of PAR energy that is available for interception and absorption. The product of FAPAR and PAR determines the amount of energy diverted to the primary production process, and reflects the combined influence of vegetation cover and solar climate.

Global patterns of incident and absorbed PAR can be effectively estimated and monitored on a global basis using satellite remote sensing techniques [Dye and Goward, 1993]. This paper reports on an initial examination of the global space-time patterns in global incident PAR and terrestrial APAR.

2. Data and Methods

2.1 Incident PAR

A data set consisting of monthly total of incident PAR was produced in earlier work [Dye, 1992, Dye and Shibasaki, 1995] using 370 nm reflectivity measurements from the Nimbus-7 Total Ozone Mapping Spectrometer (TOMS) [Eck and Dye, 1991]. The data set's original spatial resolution of 1° x 1.25° (latitude x longitude) was changed to 1° x 1° for consistency with the FAPAR data set. The resolution change was made by computing the spatially weighted average of each original-resolution grid cell overlapping each 1° x 1° grid cell. This study considers only latitudes between 60°N and 60°S to avoid inconsistencies among months caused by missing or possible ice or snow-contaminated observations at higher latitudes. The surface area in this latitudinal region is 4.47 x 10^8 km^2, or approximately 86% of the total global surface area of 5.20 x 10^8 km^2. The time coverage available from Nimbus-7 TOMS covers more than 14-years from November 1978 until March 1993. The performance of the TOMS instrument, however, declined after 1989. This study examines data from the period 1979 to 1989.

2.2 PAR-Absorption Capacity of Vegetation Cover

Field and modeling studies have demonstrated that a strong, near-linear relationship exists between remote sensing-derived measurements the normalized difference vegetation index (NDVI) and FAPAR. The time-series, global-coverage NDVI estimates available from the NOAA AVHRR sensor provide an effective means for estimating FAPAR on a global basis [Dye and Goward, 1993]. An existing global data set of monthly FAPAR values was adopted for this study. The FAPAR data set was produced by Mr. Sietse Los and others at NASA Goddard Space Flight Center as part of the International Satellite Land Surface Climatology Project (ISLSCP) Initiative I data collection effort [Sellers et al., 1994]. Global FAPAR data from this source are currently available for two years, 1987 and 1988. Monthly averages for these years were averaged for this analysis. Because FAPAR patterns are assumed invariant, any observed variations in APAR are attributable to variations in incident PAR..

Although a decadal scale global archive of calibrated NDVI measurements from the AVHRR is available, application of the data to monitoring interannual variations in FAPAR is hindered by difficulties in separating the residual effects of clouds and other atmospheric sources of contamination (aerosols, water vapor) from real changes in vegetation properties. The problem is particularly acute in seasonally or perennially moist subtropical and tropical regions, where persistent cloudcover reduces the effectiveness time-composite methods for reducing cloud contamination. It is noteworthy that whereas atmospheric effects constitute noise for the NDVI, they constitute the target signal in the TOMS UV reflectivity data since they account for variation in atmospheric transmission of PAR. Until the problem of atmospheric effects on global, time-series NDVI observations can be further resolved, it is likely that subtle variations in incident PAR may be detected with greater certainty than subtle variations in FAPAR, at least for snow and ice-free surface conditions.

3. Results and Discussion

3.1 Incident PAR

The potential (clear-sky) distribution of annual total PAR at the Earth's surface is determined by seasonal variations in Earth-sun distance and latitudinal and seasonal variations in sun-earth geometry. In the absence of variable clouds and aerosols, incident PAR would decrease as even gradient from the tropics to the poles. Seasonal and geographic variations in clouds and aerosols, however, interact with the potential pattern, resulting in the observed distribution of annual total PAR (Fig. 1) and space-time dynamics (Fig. 2a). In the equatorial regions, perennially abundant cloud cover substantially reduces PAR at the surface relative to the global maximum potential amount. The greatest annual amounts of PAR are received at

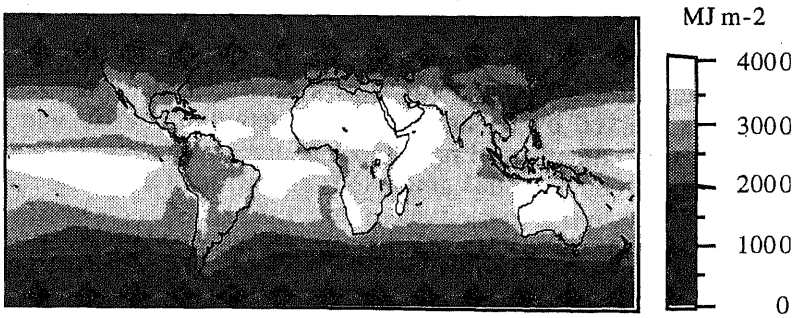

Figure 1. Mean of annual total PAR for years 1979 to 1989, excluding 1982 and 1983. Estimates are based on 370 nm reflectivity data from Nimbus-7 TOMS.

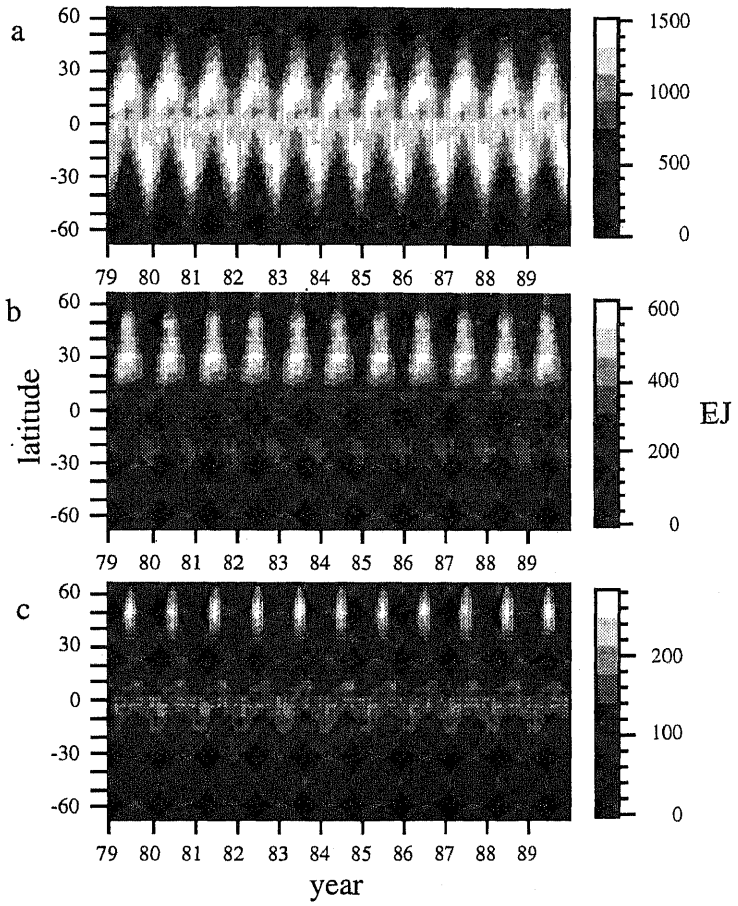

Figure 2. Temporal and latitudinal variation in monthly 1° zonal totals of (a) incident PAR, (b) terrestrial incident PAR, and (c) terrestrial absorbed PAR (APAR).

subtropical latitudes in zones characterized by atmospheric subsidence. These areas are associated with major arid regions of the globe.

For the 11-year observation period, the mean of the total annual PAR received at the Earth's surface (60°N-60°S) is 1.259 x 10^6 EJ (1 EJ = 10^{18} J). The minimum value of 1.250 x 10^6 EJ occurred in 1982, and the maximum value of 1.263 x 10^6 EJ occurred in 1986. These values represent the maximum energy available annually for use in photosynthesis and primary production. The effective incident PAR, however, would be less than the total incident PAR

when taking into account PAR received when photosynthesis is restricted by freezing temperatures.

The time series of annual total global PAR shows no strong decadal trend (Fig. 3a). The year 1982, however, is marked by an anomalous reduction in PAR, which is particularly pronounced in the northern hemisphere (Fig. 3a,b). At least two events of global significance occurred in 1982 that may account for this anomalous reduction. One is the onset of a major El Niño/Southern Oscillation event that carried over into 1983. ENSO conditions are characterized in part by regional changes in cloudiness, notably a shift in cloud cover (and sea surface temperature) from the western to the eastern tropical Pacific Ocean. Another notable event in 1982 was the eruption of Mexico's El Chichón volcano, which released a large volume of aerosol material into the atmosphere and reduced the transmissivity of the atmosphere.
From an analysis of the geographic distribution of yearly anomalies in annual total PAR relative to a 1979-1989 base period (excluding 1982 and 1983), the maximum observed deviations occur in 1982 and 1983 in the tropical Pacific Ocean (Fig. 4). The large negative anomaly in the tropical Pacific Ocean in 1983 is evidently counterbalanced by positive anomalies in other regions, such that the effect on the global total PAR is less than in 1982. The observed PAR anomalies in the tropical Pacific Ocean are generally consistent with the cloudcover shifts associated with ENSO conditions. Possible teleconnections of anomalies in other regions to ENSO conditions requires additional investigation. Atmospheric mixing may cause the potential effects of El Chichón aerosols to be more spatially homogeneous than ENSO effects, particularly over the annual periods represented here, and thus less readily detectable in the anomaly maps.

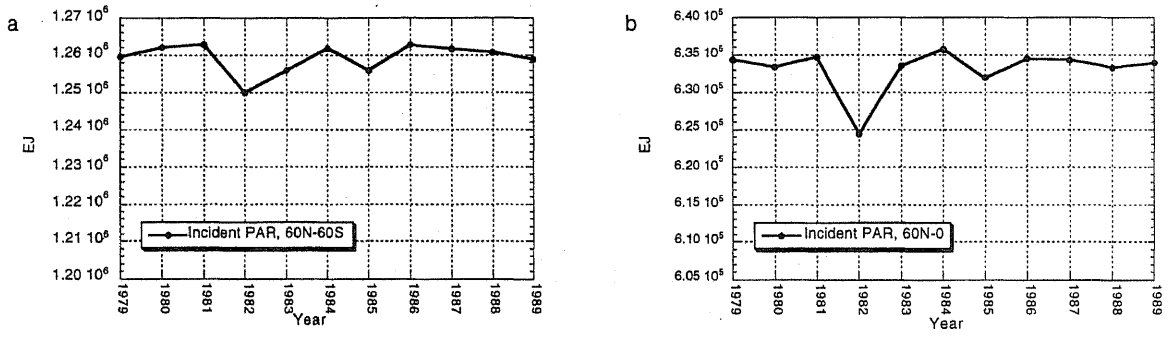

Figure 3. Time series (1979-1989) of annual total surface-incident PAR for (a) 60°N to 60°S and (b) 60°N to 0° (northern hemisphere).

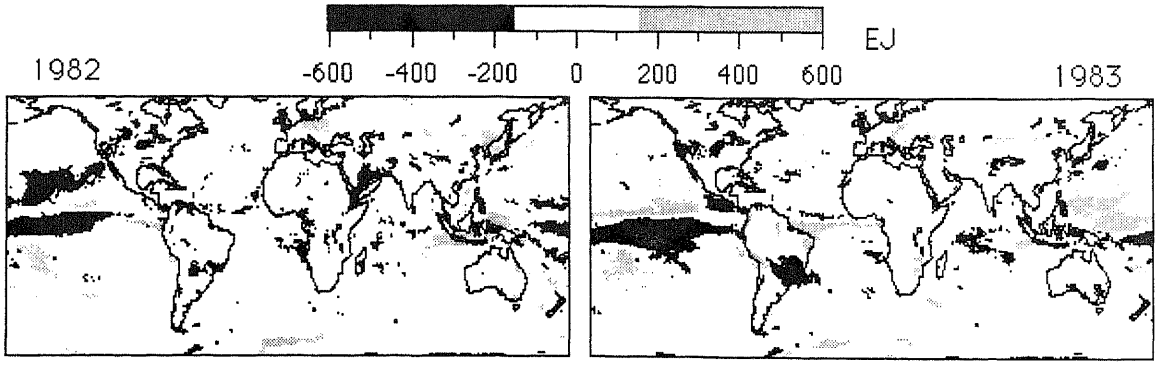

Figure 4. Anomalies in 1982 (left) and 1983 (right) in the annual total PAR per 1° grid cell, relative to base period for 1979-1989, excluding 1982-83.

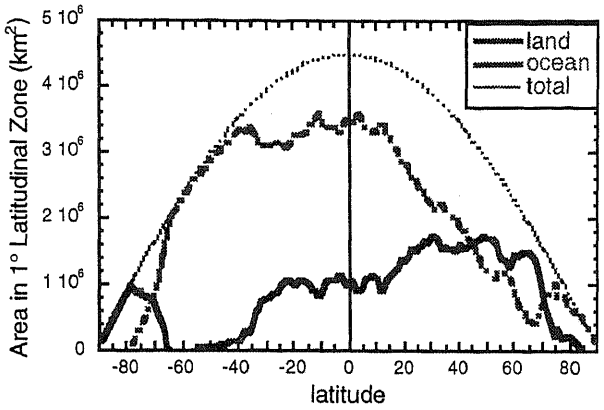

Figure 5. Variation in the total surface area within 1° latidudinal zones for land, ocean and combined (land + ocean) surfaces.

3.2 Ocean and Terrestrial-incident PAR

The calculated 11-year (1979-1989) means of annual total PAR incident for the terrestrial and ocean surfaces (60°N-60°S) are 3.42 x 10^5 EJ (27% of total) and 9.17 x 10^5 EJ (73% of total), respectively. These calculations involved reference to Matthews' [1983] global 1° vegetation map for discriminating land and ocean areas. The key factors that influence this distribution between land and ocean are the proportion and latitudinal distribution of land and ocean surface areas (Fig. 5), and land-ocean differences in cloud cover distribution and seasonality.

The geographical configuration of the land masses and associated seasonal cloud patterns causes the space-time pattern of terrestrial incident PAR (Fig. 2b) to diverge markedly from the global (land + ocean) pattern (Fig. 2a). The proportion of land in southern hemisphere latitudes declines rapidly from about 23% in the tropic zone to 0% near 55°S latitude, which marks the southernmost extent of the South American continent. No significant land area occurs between 55°S and the beginning of the Antarctic continent at approximately 64°S. South of the southern extent of Australia at about 40°S latitude, terrestrial incident PAR is limited primarily to that intercepted by southern Argentina and Tierra del Fuego in South America, and is absent altogether below 55°S latitude in the 60°N-60°S study area (Fig. 2b). In both proportional and absolute terms, the greatest land surface areas occur at middle latitudes in the northern hemisphere, between about 15°N and 50°N (Fig. 5). In this region of the northern hemisphere, land comprises between about 40% to 60% of the total zonal surface area. The highest annual amounts of terrestrial incident PAR occur in this region. A distinct global peak of between 500 and 600 EJ per 1° latitude occurs in the summer months near 30°N. This peak is attributable to the combination of extensive land area coincident with the occurrence of zones of atmospheric subsidence associated with major desert or arid regions. The strong latitudinal contrast in the seasonality of terrestrial incident PAR is also apparent. Tropical latitudes are characterized by a steady monthly rate of energy receipt, with seasonality increasing steadily with increasing latitude.

Separation of the global total annual PAR figures into ocean and terrestrial components permits their interannual dynamics to be evaluated independently. The time patterns of incident PAR for land and ocean areas (Fig. 6) suggest that the 1982-83 ENSO event (and possibly El Chichón) had a pronounced effect on the PAR regime in both ocean and terrestrial environments. The likely source for the anomalous reduction in terrestrial PAR is observed in 1985 (Fig. 6b,d) cause remains to be identified.

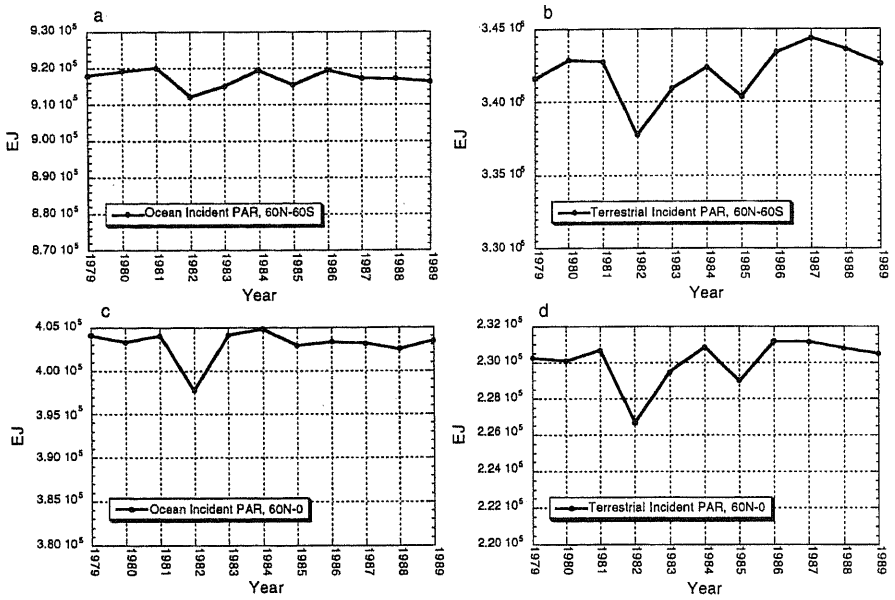

Figure 6. Time series for 1979-1989 of annual total incident PAR for (a) ocean surfaces (60N-60S), (b) terrestrial surfaces (60N-60S), (c) northern hemisphere oceans (0°-60°S), and (d) northern hemisphere terrestrial surfaces (0°-60°N).

3.3 Terrestrial Absorbed PAR

The analysis indicates that terrestrial vegetation between 60°N and 60°S latitudes intercepts and absorbs an average of 1.10 x 10^5 EJ PAR annually (mean for 1979-1989). This amount corresponds to 8.8% of the global total incident PAR and 32.3% of the total terrestrial incident PAR in this latitude zone. During the 11-year study period, annual terrestrial APAR varied from a minimum of 1.09 x 10^5 EJ in 1982 to a maximum of 1.12 x 10^5 EJ in 1987, corresponding to a dynamic range of 0.03 x 10^5 EJ or 2.7% of the 11-year mean. These figures assume the no interannual variation in monthly FAPAR patterns, as discussed earlier.

By definition, APAR at a given location and time is dependent on the simultaneous magnitude of FAPAR and PAR (Fig. 7). In effect, each variable scales the other. High incident PAR coincident with low FAPAR (e.g. a low or mid-latitude desert) produces low APAR. Conversely, high incident PAR coincident with high FAPAR produces high APAR (e.g, lush, irrigated croplands in an arid region). Global patterns in APAR thus cannot be reliably predicted from knowledge of either FAPAR or PAR alone.

The combination of discrete FAPAR and incident PAR patterns results in a space-time pattern for APAR (Fig. 2c) that is distinct from the component FAPAR and PAR patterns (Fig. 2a,b) [Dye and Goward, 1993]. The equatorial belt between approximately 10°N and 10°S latitude is characterized by perennially consistent, moderate zonal average rates of terrestrial APAR (150-200 MJ m^{-2} mo^{-1}). The global maximum rates occur in the middle latitudes the northern hemisphere summer months (200-280 MJ m^{-2} mo^{-1}). The relative paucity of vegetation cover relative to available PAR and land surface area in the subtropical belt between about 10°N and 30° N latitudes results in a relatively low zonal average APAR (50-100 MJ m^{-2} mo^{-1}). These latitudes of low photosynthetic activity form in effect a geographical buffer zone between the seasonally intensive productivity in the northern temperate latitudes and the perennially productive tropics.

The time series of annual total terrestrial APAR (60°N-60°S) exhibits notable interannual variation (Fig. 8). The influence of the ENSO and possibly El Chichón-related reduction in incident PAR on terrestrial APAR in 1982 is evident. The time series pattern of terrestrial incident PAR and terrestrial APAR, however, are distinct from one another. Although the monthly FAPAR patterns are fixed in this analysis, it is reasonable for the incident PAR and APAR time patterns to be unique. The differences may arise from interannual variations in spatial distribution of incident PAR over the fixed monthly FAPAR fields. A common time pattern would be expected only in the unlikely scenario that variations in incident PAR are perfectly and positively correlated in location and time with the fixed monthly variations in FAPAR.

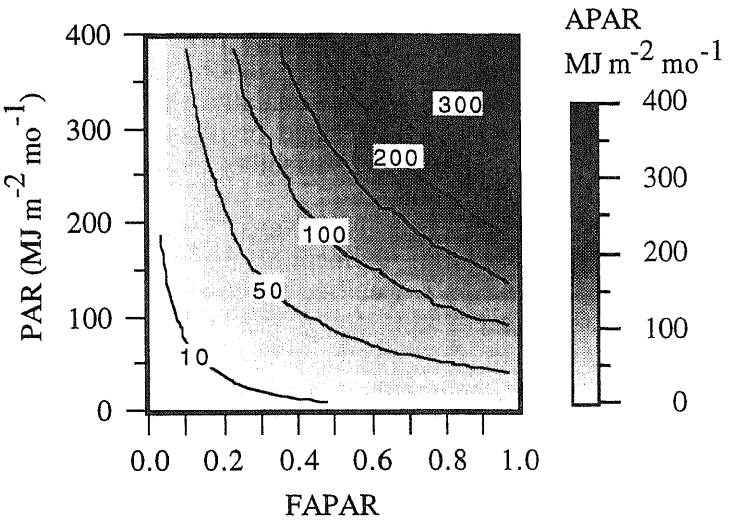

Figure 7. Variation in APAR (contours and gray levels) as a function of monthly incident PAR and FAPAR.

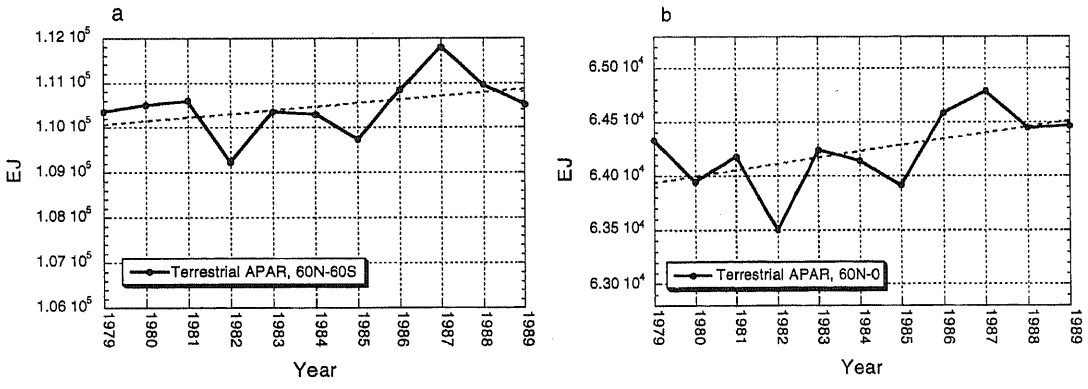

Figure 8. Annual variability in terrestrial APAR for (a) global land areas (60°N-60°S), and (b) the northern hemisphere land areas (60°N-0°). The dashed lines indicate the line of least-squares from linear regression.

A decadal-scale trend toward increasing terrestrial APAR is evident over a dominant portion of the 11-year observation period. Based on line of least squares from linear regression, terrestrial APAR increased at an average rate of 79.7 EJ y^{-1}, corresponding to a proportional increase of approximately 0.07% per year. A slightly stronger trend is evident when considering only the northern hemisphere, where the rate is 57.56 EJ y^{-1}, or approximately 0.9% of the 11-year mean northern hemisphere terrestrial APAR value of 6.42 x 10^4 EJ y^{-1}. The significance and reliability these statistical trends, their relation to other climate indices and biospheric functioning are currently under investigation.

4. Discussion and Conclusions

The results reported in this paper constitute a first satellite-based examination of the global receipt and biological diversion of photosynthetically active radiation. The observed patterns define the energy basis for global primary production and biospheric functioning. The observed interannual variations and trends, if confirmed, may have significant influence on global patterns of primary production. This influence may occur directly through fluctuations in the energy flow to photosynthesis, and indirectly through relations to other climatic variables, such as temperature and precipitation, that influence growth and production.

A limitation of the present analysis is the lack of accounting for possible interannual variations in FAPAR. Removal of cloud contamination from time-series NDVI observations while maintaining sensitivity to real variations in vegetation conditions is a vexing problem in remote sensing, particularly in seasonally or perennially cloud-prone regions. Time-series global NDVI data that are sufficiently free of cloud or other atmospheric contamination are critical to enable reliable detection of interannual variability in FAPAR.

Incident PAR and APAR data are typically required for application to physically based, mechanistic models of primary production. Incident or absorbed PAR may be used to predict rates of canopy photosynthesis based on a specified photosynthetic light-response curve [e.g., Goward and Dye, 1987] or by accounting for the overall "efficiency" with which time-integrated APAR is converted to dry matter [e.g., Prince et al., 1991]. Reliable parameterization of such models over the global range of vegetation physiognomic types and climatic conditions, however, remains a major research challenge. Given presently large uncertainties in such parameterizations, the satellite estimates of the global energy flow into primary production described here may be among the variables in which the most confidence may currently be placed. Additional research is in progress to provide additional validation and refinement of the satellite PAR and FAPAR measurements, and to achieve an improved quantitative assessment of the distribution and dynamics of global ocean and terrestrial productivity.

5. References

Dye, D.G., 1992. Satellite estimation of the global distribution and interannual variability of photosynthetically active radiation. Ph.D. dissertation, University of Maryland, College Park.

Dye, D.G., and Goward, S.N., 1993, Absorption of photosynthetically active radiation by global land vegetation in August 1984. *International Journal of Remote Sensing*, 14(18):3361-3364.

Dye, D. G., and Shibasaki, R., 1995, Intercomparison of global PAR data sets. *Geophysical Research Letters*, 22(15):2013-2016.

Eck, T.F., and Dye, D.G., 1991. Satellite estimation of incident photosynthetically active radiation using ultraviolet reflectance. Remote Sensing of Environment, 38:135-146.

Goward, S.N., and Dye, D.G., 1987, Evaluating North American primary productivity with satellite observations. *Advances in Space Research*, 7:165-174.

Prince, S.D., 1991, A model of regional primary production for use with coarse resolution satellite data. *International Journal of Remote Sensing*, 12:1313-1330.

Sellers, P.J., S.O. Los, C.J. Tucker, C.O. Justice, D.A. Dazlich, G.J. Collatz, and D.A. Randall, 1994. A global 1 by 1 degree NDVI data set for climate studies. Part 2: The generation of global fields of terrestrial biophysical parameters from the NDVI. *International Journal of Remote Sensing*, 15(17):3519-3545.